

# A Self-Assembled Organometallic Sphere: $[\{(t\text{-BuC}_5\text{H}_4)(t\text{-BuC}_5\text{H}_3)\text{Zr}(\mu\text{-H})\text{Na}\}_2]_4$

Yuzhong Wang, Brandon Quillian, Pingrong Wei, Chaitanya S. Wannere,  
 Paul v. R. Schleyer, and Gregory H. Robinson\*

Department of Chemistry and the Center for Computational Chemistry,  
 The University of Georgia, Athens, Georgia 30602-2556

Received February 27, 2006

**Summary:** Sodium reduction of  $(t\text{-BuC}_5\text{H}_4)_2\text{ZrCl}_2$  in diethyl ether gives  $[\{(t\text{-BuC}_5\text{H}_4)(t\text{-BuC}_5\text{H}_3)\text{Zr}(\mu\text{-H})\text{Na}\}_2 \cdot \text{OEt}_2]_2$ , **1**; toluene extraction of **1** produces the self-assembled tetramer  $[\{(t\text{-BuC}_5\text{H}_4)(t\text{-BuC}_5\text{H}_3)\text{Zr}(\mu\text{-H})\text{Na}\}_2]_4$ , **2** (the  $\text{Na}_8\text{Zr}_8$  linkage of **2** resembles the seams of a “tennis ball”). Both **1** and **2** are diamagnetic, which may be attributed to the presence of direct Zr–Zr bonds (Zr–Zr: 3.2930(16) Å (**1**), 3.3076(7) Å (**2**)).

## Introduction

Promising applications in synthesis, catalysis, and materials<sup>1–6</sup> encourage the construction of well-defined molecular capsules and cages.<sup>6–12</sup> Can three-dimensional hollow architectures involving organometallic transition metal compounds be achieved via self-assembly? While many organometallic macrocycles have been obtained by this “bottom-up” synthetic technique, examples of the self-assembly of three-dimensional organometallic molecules with inner cavities are scant.<sup>2,3,13,14</sup> We now report the synthesis and molecular structure of the self-assembled organometallic sphere  $[\{(t\text{-BuC}_5\text{H}_4)(t\text{-BuC}_5\text{H}_3)\text{Zr}(\mu\text{-H})\text{Na}\}_2]_4$  (**2**), consisting of anionic, low-valent zirconocene hydrides.

## Results and Discussion

The recent conversion of dinitrogen to ammonia utilizing low-valent zirconocene derivatives<sup>15</sup> further increased our enthusiasm for exploring the chemistry of low-valent group 4 transition

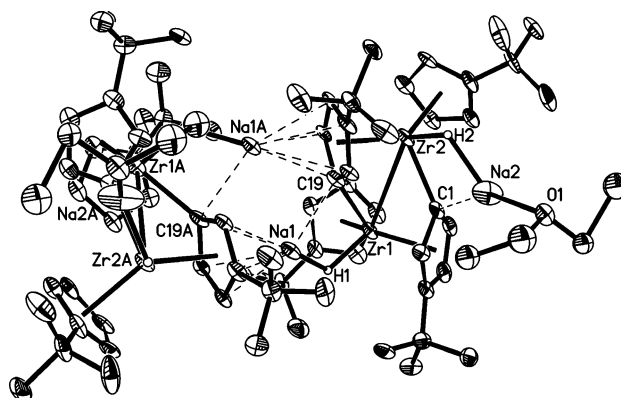
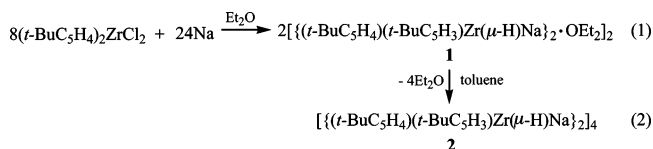


**Figure 1.** Molecular structure of **1** (thermal ellipsoids shown at the 30% probability levels; hydrogen atoms on carbon omitted for clarity). Selected bond lengths (Å) and angles (deg): Zr(1)–Zr(2) 3.2930(16), Zr(1)–C(19) 2.358(11), Zr(1)–H(1) 1.86(11), Zr(2)–C(1) 2.335(11), Zr(2)–H(2) 1.85(13); C(1)–Zr(2)–Zr(1) 45.1(3), C(19)–Zr(1)–Zr(2) 46.7(2), H(1)–Zr(1)–Zr(2) 128(3), H(2)–Zr(2)–Zr(1) 122(3).

metal complexes.<sup>16,17</sup> Indeed, sodium metal reduction of  $(t\text{-BuC}_5\text{H}_4)_2\text{ZrCl}_2$  in  $\text{Et}_2\text{O}$  led to the formation of very air- and moisture-sensitive red crystals of  $[\{(t\text{-BuC}_5\text{H}_4)(t\text{-BuC}_5\text{H}_3)\text{Zr}(\mu\text{-H})\text{Na}\}_2 \cdot \text{OEt}_2]_2$ , **1** (Figure 1) (eq 1).



X-ray analysis of **1** reveals a dimeric  $\{(t\text{-BuC}_5\text{H}_4)(t\text{-BuC}_5\text{H}_3)\text{Zr}(\mu\text{-H})\text{Na}\}_2 \cdot \text{OEt}_2$  structure with  $C_2$  symmetry. The monomeric units are bound ionically by  $\text{Na}^+$  interactions with the  $t\text{-BuC}_5\text{H}_3$  ligand in an  $\eta^5$ -fashion. The charges of the dinuclear and dianionic zirconocene hydride moieties in each  $\{(t\text{-BuC}_5\text{H}_4)(t\text{-BuC}_5\text{H}_3)\text{Zr}(\mu\text{-H})\text{Na}\}_2 \cdot \text{OEt}_2$  unit are balanced by two  $\text{Na}^+$  cations. The coordination of  $\text{Et}_2\text{O}$  to the terminal  $\text{Na}^+$  cations is important in stabilizing the dimer. We suspected that interesting, perhaps more complex aggregates might self-assemble in the absence of such  $\text{Et}_2\text{O}$ -stabilized coordination. Indeed, our successful isolation of the  $\text{Et}_2\text{O}$ -free tetrameric **2**, by toluene extraction of **1** (eq 2), realized this expectation.

Isolated as air- and moisture-sensitive dark red crystals, **2** exhibits remarkably high thermal stability (mp 305–307 °C).

\* To whom correspondence should be addressed. E-mail: robinson@chem.uga.edu.

(1) MacGillivray, L. R.; Atwood, J. L. *Angew. Chem., Int. Ed.* **1999**, *38*, 1018–1033.

(2) Leininger, S.; Olenyuk, B.; Stang, P. J. *Chem. Rev.* **2000**, *100*, 853–907.

(3) Seidel, S. R.; Stang, P. J. *Acc. Chem. Res.* **2002**, *35*, 972–983.

(4) Lutzen, A. *Angew. Chem., Int. Ed.* **2005**, *44*, 1000–1002.

(5) Vriezema, D. M.; Aragones, M. C.; Elemans, J. A. A. W.; Cornelissen, J. J. L. M.; Rowan, A. E.; Nolte, R. J. M. *Chem. Rev.* **2005**, *105*, 1445–1489.

(6) Rebeck, J., Jr. *Angew. Chem., Int. Ed.* **2005**, *44*, 2068–2078.

(7) Beissel, T.; Powers, R. E.; Raymond, K. N. *Angew. Chem., Int. Ed. Engl.* **1996**, *35*, 1084–1086.

(8) Hartshorn, C. M.; Steel, P. J. *Chem. Commun.* **1997**, 541–542.

(9) Abrahams, B. F.; Egan, S. J.; Robson, R. J. *Am. Chem. Soc.* **1999**, *121*, 3535–3536.

(10) Takeda, N.; Umemoto, K.; Yamaguchi, K.; Fujita, M. *Nature* **1999**, *398*, 794–796.

(11) Olenyuk, B.; Whiteford, J. A.; Fechtenkotter, A.; Stang, P. J. *Nature* **1999**, *398*, 796–799.

(12) Atwood, J. L.; Barbour, L. J.; Jerga, A. *Chem. Commun.* **2001**, 2376–2377.

(13) Klausmeyer, K. K.; Rauchfuss, T. B.; Wilson, S. R. *Angew. Chem., Int. Ed.* **1998**, *37*, 1694–1696.

(14) Sun, S.-S.; Lees, A. J. *Chem. Commun.* **2001**, 103–104.

(15) Pool, J. A.; Lobkovsky, E.; Chirik, P. J. *Nature* **2004**, *427*, 527–530.

(16) Yang, X.-J.; Quillian, B.; Wang, Y.; Wei, P.; Robinson, G. H. *Organometallics* **2004**, *23*, 5119–5120.

(17) Wang, Y.; Quillian, B.; Yang, X.-J.; Wei, P.; Chen, Z.; Wannere, C. S.; Schleyer, P. v. R.; Robinson, G. H. *J. Am. Chem. Soc.* **2005**, *127*, 7672–7673.

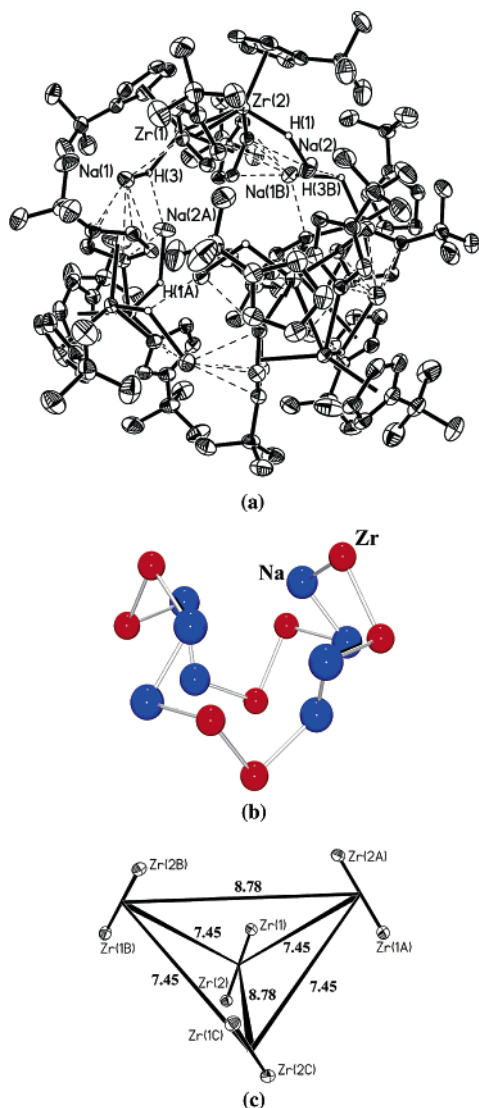


**Figure 2.** (a) Molecular structure of **2** (thermal ellipsoids are shown at the 30% probability levels; hydrogen atoms on carbon are omitted for clarity). Selected bond lengths (Å) and angles (deg): Zr(1)–Zr(2) 3.3076(7), Zr(1)–H(3) 1.94(6), Zr(2)–H(1) 1.91(5); Zr(2)–Zr(1)–H(3) 128.3(18), Zr(1)–Zr(2)–H(1) 129.9(14). (b)  $\text{Na}_8\text{Zr}_8$  “linkage” of **2** (bridging ligands are omitted for clarity). (c) Approximately tetrahedral cavity of **2** (side lengths of the cavity are in Å).

X-ray analysis shows that the ligand-bridged  $\text{Na}_8\text{Zr}_8$  metallic framework of **2** (Figure 2a) results in a hollow spherical structure. Interestingly, the  $S_4$  symmetry and the shape of the  $\text{Na}_8\text{Zr}_8$  “linkage” resemble the seams of a tennis ball (Figure 2b). The midpoints of the four Zr–Zr moieties in this “molecular tennis ball” are oriented tetrahedrally (Figure 2c). Based on the 7.45, 7.45, and 8.78 Å lengths of the sides of each face, the volume of the roughly tetrahedral inner cavity of **2** is calculated to be ca. 53 Å<sup>3</sup>. The quasi-sphere **2** has a diameter of ca. 16.1 Å (as defined by the *t*-BuC<sub>5</sub>H<sub>4</sub> ligand hydrogen separations) and encloses a volume of 2185 Å<sup>3</sup>.

Compound **2** is a tetramer of the  $\{(t\text{-BuC}_5\text{H}_4)(t\text{-BuC}_5\text{H}_3)\text{Zr}(\mu\text{-H})\text{Na}\}_2$  subunit, **3** (Figure 3a). The aggregation involves two ionic bonding arrangements (Figure 2a): (1)  $\eta^5$ -coordination of Na<sup>+</sup> cations to bridging *t*-BuC<sub>5</sub>H<sub>3</sub> rings and (2) Na<sup>+</sup> cation interaction with a hydride of the neighboring subunit. In contrast, the **1** ensemble involves only the  $\eta^5$  Na<sup>+</sup>–*t*-BuC<sub>5</sub>H<sub>3</sub> interaction (Figure 1). Consequently, the spatial orientation relationships of the neighboring subunits in **2** and **1** differ.

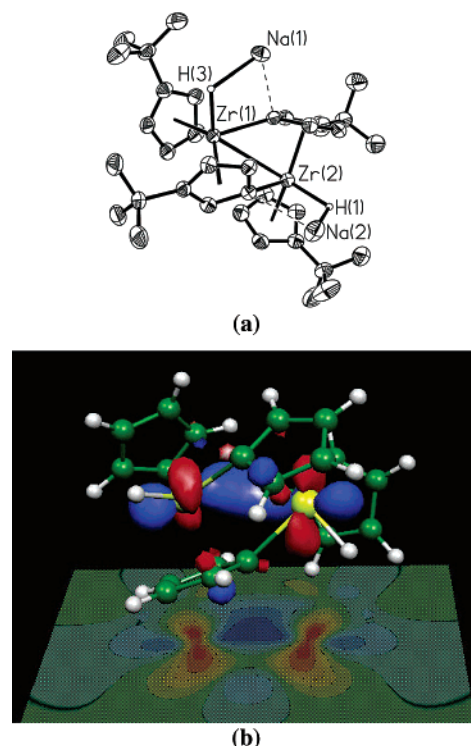


**Figure 3.** (a) Structure of the subunit **3** of complexes **1** and **2** (thermal ellipsoids shown at the 30% probability levels; hydrogen atoms on carbon omitted for clarity). (b) Representation of the HOMO of **3Cp** (sodium atoms are omitted for clarity).

The dimeric unit **3** is common to both complexes **1** and **2**. Each of the monomeric subunits of **3** adopts a staggered conformation. Besides being both  $\pi$ - and  $\sigma$ -coordinated by the bridging *t*-BuC<sub>5</sub>H<sub>3</sub> ligands, each zirconium also is  $\pi$ -bonded to a free *t*-BuC<sub>5</sub>H<sub>4</sub> ligand and  $\sigma$ -bonded to a hydride-hydrogen. The structure of subunit **3** (Figure 3a) supports the ring-to-metal hydrogen migration, as does the observed Zr–H absorption band (at 1200–1510 cm<sup>−1</sup>).<sup>18</sup> The two hydrides in the subunit **3** bridge the zirconium and sodium atoms. All of the Zr–H bond distances in **1** (1.85(13) and 1.86(11) Å) and **2** (1.91(5) and 1.94(6) Å) are within the reported 1.73(7)–2.26(8) Å range.<sup>19</sup> The “bridging” character of the hydride ligands also was confirmed by <sup>1</sup>H NMR spectroscopy. The  $\delta$  <sup>1</sup>H Zr–H resonances of **1** and **2**, at −2.36 and −2.71 ppm, respectively, are close to the −3.17 ppm reported for [(CpCMe<sub>3</sub>)<sub>2</sub>Zr( $\mu$ -H)H]<sub>2</sub><sup>19</sup> and the −1.66 ppm value computed for the  $\{(\text{Cp})(\text{C}_5\text{H}_4)\text{Zr}(\mu\text{-H})\text{Na}\}_2$  (**3Cp**) model of **3**.<sup>20</sup> Note that the sodium cation also interacts with the *t*-BuC<sub>5</sub>H<sub>3</sub> ligand in an  $\eta^1$ -fashion.

The d<sup>1</sup> electronic configuration of zirconium in **1** and **2** corresponds to a formal oxidation state of III. However, both **1** and **2** are diamagnetic, with 3.2930(16) and 3.3076(7) Å Zr–Zr distances, respectively. Zirconium–zirconium bond distances have been reported for the range 3.099(2)–3.3608(8) Å.<sup>21,22</sup> However, the Zr–Zr distance may be perturbed by the steric constraints imposed by the bridging *t*-BuC<sub>5</sub>H<sub>3</sub> ligands. Hence, a simplified model (**3Cp**) of the subunit **3** of **1** and **2** was computed at the B3LYP/LANL2DZ DFT level.<sup>23</sup> Similar to subunit **3**, the optimized **3Cp** minimum<sup>23</sup> has C<sub>2</sub> symmetry and two staggered (Cp)(C<sub>5</sub>H<sub>4</sub>)Zr( $\mu$ -H)Na fragments. The computed

(18) Pez, G. P.; Putnik, C. F.; Suib, S. L.; Stucky, G. D. *J. Am. Chem. Soc.* **1979**, *101*, 6933–6937.

(19) Larssonneur, A. M.; Choukroun, R.; Jaud, J. *Organometallics* **1993**, *12*, 3216–3224.

Zr–Zr distance (3.314 Å) in **3Cp** agrees well with the experimental Zr–Zr values for **1** and **2**. The computed 1.965 Å Zr–H distance for **3Cp** fits **2** (1.91(5) and 1.94(6) Å) better than **1** (1.85(13) and 1.86(11) Å), but lies within or near the experimental uncertainty ranges.

The **3Cp** HOMO (see Figure 3b) describes the Zr–Zr  $\sigma$ -bonding orbital (the high-lying LUMO+5<sup>23</sup> is its antibonding counterpart). Similar to the bent Ti–Ti bond in [Cp( $\mu$ - $\eta^1$ : $\eta^5$ -C<sub>5</sub>H<sub>4</sub>)Ti(PMe<sub>3</sub>)<sub>2</sub>]<sub>2</sub>,<sup>24</sup> this HOMO shows a distinctly bent Zr–Zr  $\sigma$ -bond, which may be attributed to the strain effect of the bridging ligands.<sup>24</sup> The Wiberg bond index, WBI, value of 0.453 for the Zr–Zr interaction (given by natural bond orbital (NBO) analysis) supports the presence of a Zr–Zr bond. Notably, this bond order value for the Zr–Zr interaction is comparable to Mo–Mo bond orders, 0.328 and 0.333, reported for [Mo( $\eta^5$ -Cp)(CO)<sub>3</sub>]<sub>2</sub> and [Mo( $\eta^5$ -Cp)(CO)<sub>2</sub>]<sub>2</sub>( $\mu$ -PMe<sub>2</sub>), respectively.<sup>25</sup> Thus, we attribute the diamagnetism of **1** and **2** to the direct Zr–Zr bonding in these 18-electron compounds.

The self-assembly of the title compound will be used as a benchmark as we continue these studies.

### Experimental Section

All reactions were performed under purified argon using Schlenk techniques in conjunction with an inert atmosphere drybox (MBraun LabMaster 130). (*t*-BuC<sub>5</sub>H<sub>4</sub>)<sub>2</sub>ZrCl<sub>2</sub> was purchased from Strem Chemical Co. and used as received. Solvents were dried and collected under nitrogen using an MBraun MB-SP Series solvent purification system. <sup>1</sup>H NMR spectra were recorded on a Bruker AC-300 spectrometer. IR spectra were recorded on a Nicolet-AVATAR 360 FT-IR ESP spectrometer. Elemental analyses were performed by Complete Analytical Laboratory, Inc. (Parsippany, NJ).

**Synthesis of 1 and 2.** (a) Under an inert atmosphere of dry argon, 60 mL of diethyl ether was added to a flask containing (*t*-BuC<sub>5</sub>H<sub>4</sub>)<sub>2</sub>ZrCl<sub>2</sub> (1.00 g, 2.472 mmol) and finely cut sodium (0.25 g, 10.870 mmol) at ambient temperature. After being powerfully stirred over 5 days, the dark purple-red solution was filtered. The filtrate was concentrated to 5 mL and then kept standing at ambient temperature. Over 4 days, red crystals of **1** (0.31 g, 32% yield) were observed. Mp: 281–284 °C. <sup>1</sup>H NMR (THF-*d*<sub>8</sub>):  $\delta$  –2.36 (s, 4H, Zr–H–Na), 1.12 [t, 12H, (CH<sub>3</sub>CH<sub>2</sub>)<sub>2</sub>O], 1.18 (s, 36H, *t*-Bu), 1.33 (s, 36H, *t*-Bu), 3.39 (q, 8H, (CH<sub>3</sub>CH<sub>2</sub>)<sub>2</sub>O), 3.93 (bd, 4H, Cp), 4.41 (q, 4H, Cp), 4.53 (q, 4H, Cp), 4.60 (q, 4H, Cp), 4.82 (t, 4H, Cp), 5.10 (t, 4H, Cp), 5.29 (q, 4H, Cp). IR (cm<sup>–1</sup>, KBr):  $\nu$  (Zr–H) = 1200–1510. Anal. (CALI, Parsippany, NJ) Calcd (found) for C<sub>80</sub>H<sub>124</sub>O<sub>2</sub>Na<sub>4</sub>Zr<sub>4</sub> (1574.69): C, 61.02 (60.84); H, 7.94 (7.79). (b) **1** (0.50 g) was extracted by using toluene. After filtration, the toluene solution

was concentrated to 5 mL and kept standing at ambient temperature. Over one week, dark red crystals of **2** (0.25 g, 56% yield) were observed. Mp: 305–307 °C. <sup>1</sup>H NMR (THF-*d*<sub>8</sub>):  $\delta$  –2.71 (s, 8H, Zr–H–Na), 1.09 (s, 72H, *t*-Bu), 1.41 (s, 72H, *t*-Bu), 3.67 (bs, 8H, Cp), 4.53 (m, 24H, Cp), 5.12 (bd, 8H, Cp), 5.35 (bs, 8H, Cp), 5.66 (bs, 8H, Cp). IR (cm<sup>–1</sup>, KBr):  $\nu$  (Zr–H) = 1200–1510. Anal. Calcd (found) for C<sub>158</sub>H<sub>224</sub>Na<sub>8</sub>Zr<sub>8</sub> (3037.18): C, 62.48 (62.59); H 7.43 (7.19).

**X-ray Crystal Structure Determination of 1 and 2.** Crystals of **1** and **2** were mounted in glass capillaries under an atmosphere of argon in the drybox. Crystal data for **1**: C<sub>80</sub>H<sub>124</sub>O<sub>2</sub>Na<sub>4</sub>Zr<sub>4</sub>, fw = 1574.69, monoclinic, C2/c (No. 15), *a* = 33.464(12) Å, *b* = 13.172(5) Å, *c* = 19.356(7) Å,  $\beta$  = 108.274(6)°, *V* = 8101(5) Å<sup>3</sup>, *Z* = 4, *R*<sub>1</sub> = 0.0752, *wR*<sub>2</sub> = 0.1712. The X-ray intensity data were collected at 100(2) K on a Bruker SMART APEX II X-ray diffractometer system with graphite-monochromated Mo K $\alpha$  radiation ( $\lambda$  = 0.710 73 Å), using the  $\omega$ -scan technique. The structure was solved by direct methods using the SHELXTL 6.1 bundled software package.<sup>26</sup> Absorption corrections were applied with SADABS. All non-hydrogen atoms were refined anisotropically except for the disordered carbon atoms of diethyl ether, which were divided into two sets labeled as C37, C38, C39, C40 with 39.486% occupancies and C37', C38', C39', C40' with 60.514% occupancies. The corresponding hydrogen atoms of diethyl ether were added in the correct calculated positions. The two hydrides and two hydrogen atoms on C22, C23 of Cp are located from a difference Fourier map and refined. The rest of the hydrogen atom positions were calculated and allowed to ride on the attached carbon atoms with the isotropic temperature factors fixed at 1.1 times those of the corresponding carbon atoms. Crystal data for **2**: C<sub>158</sub>H<sub>224</sub>Na<sub>8</sub>Zr<sub>8</sub>, fw = 3037.18, tetragonal, *I*<sub>1</sub>/*acd* (No. 142), *a* = 30.6848(12) Å, *b* = 30.6848(12) Å, *c* = 33.474(2) Å, *V* = 31518(3) Å<sup>3</sup>, *Z* = 8, *R*<sub>1</sub> = 0.0397, *wR*<sub>2</sub> = 0.1001. The X-ray intensity data were collected at room temperature on a Bruker SMART TM CCD-based X-ray diffractometer system with graphite-monochromated Mo K $\alpha$  radiation ( $\lambda$  = 0.710 73 Å), using the  $\omega$ -scan technique. The structure was solved by direct methods using the SHELXTL 6.1 bundled software package.<sup>26</sup> Absorption corrections were applied with SADABS. All non-hydrogen atoms were refined anisotropically except for the half toluene solvent molecule with C<sub>2</sub> symmetry. The methyl group of toluene was found disordered in the 1- and 3-positions of the phenyl ring with half-occupancies of each. The two hydrides and three hydrogen atoms on one Cp group were located from a difference Fourier map and refined. Except for the hydrogen atoms of the disordered toluene, the rest of the hydrogen atom positions were calculated and allowed to ride on the attached carbon atoms with the isotropic temperature factors fixed at 1.1 times those of the corresponding carbon atoms.

**Acknowledgment.** We are grateful to the National Science Foundation (CHE-0209857) for support of this research.

**Supporting Information Available:** Full details of the computations and X-ray crystallographic studies, including a cif file. This material is available free of charge via the Internet at <http://pubs.acs.org>.

OM0601899

(26) Sheldrick, G. M. *SHELXTL 6.1*, Crystallographic Computing System; Bruker Analytical X-Ray Systems: Madison, WI, 2000.

(20) The <sup>1</sup>H chemical shift was evaluated at GIAO-PW91PW91/LANL2DZ//B3LYP/LANL2DZ. The expected absolute proton shieldings,  $\sigma$ , were converted to chemical shifts,  $\delta$ , as the difference from proton shieldings of TMS, 32.73 (computed at the same level).

(21) Cotton, F. A.; Diebold, M. P.; Kibala, P. A. *Inorg. Chem.* **1988**, *27*, 799–804.

(22) Xie, X.; Jones, J. N.; Hughbanks, T. *Inorg. Chem.* **2001**, *40*, 522–527.

(23) Computations: The structure is optimized at the DFT level (B3LYP) with the LANL2DZ basis set with the Gaussian-98 program (reference and details of the computations are in the Supporting Information).

(24) Benard, M.; Rohmer, M. M. *J. Am. Chem. Soc.* **1992**, *114*, 4785–4790.

(25) Hong, F.-E.; Chang, Y.-C. *Bull. Chem. Soc. Jpn.* **2004**, *77*, 115–121.